UNITED STATES DEPARTMENT OF THE INTERIOR

GEOLOGICAL SURVEY

Historical Shoreline Changes at Rincón, Puerto Rico

by

E. Robert Thieler[1]

and

Milton Carlo[2]

Open-File Report

95-72

14 January 1995

---

[1]Duke University, Department of Geology, Program for the Study of Developed Shorelines, Campus Box 90228, Durham, NC 27708-0228.

[2]U.S. Geological Survey, P.O. Box 5917, Pta. de Tierra Sta., San Juan, PR 00906.

CONTENTS

SUMMARY

A record of historical shoreline positions and rates-of-change has been compiled for the area near Rincón, Puerto Rico over the period 1950-1994. The study area includes approximately 8 km of the northwestern coast, from Punta Higüero to Punta Cadena. Historical shoreline positions were obtained from aerial photographs. More recent shoreline position surveys were conducted using a portable, differential GPS system.

The study area can be divided into four distinct reaches based on erosion rate. Reach A, from Punta Higüero to just south of Punta Ensenada, is characterized by long-term erosion rates <0.3 m/yr. Reach B extends from just south of Punta Ensenada to 500 m south of the Quebrada los Ramos. Erosion rates here are generally >1.0 m/yr, and reach a maximum of nearly 3.0 m/yr. Reach C, which extends from 500 m south of Quebrada los Ramos to Córcega, has an erosion rate of about 0.5 m/yr. Reach D, from Córcega to Punta Cadena, is characterized by erosion rates <0.5 m/yr.

The erosion rate data for Reach B show a profound change in the historical trend between 1977 and 1987. Prior to 1977, the erosion rate was similar to Reach C (0.5 m/yr). Over the last seven years, however, the erosion rate is more than 3.0 m/yr. This increased erosion correlates with the 1983 construction of a relatively small marina facility within Reach B. The emplacement of a breakwater/jetty system and the continued removal of dredged sediment at the marina entrance appear to be the major contributing factors to the recent increase in erosion rates.

INTRODUCTION

As development in coastal areas has increased, accurate measurements of historical shoreline changes have become a prerequisite for coastal management. Recent erosion rates and historical storm response provide a scientific basis for formulating sound coastal management policy. For example, recent erosion rates are presently used in several U.S. states to locate oceanfront construction setback lines; storm response data is used to establish post-storm reconstruction regulations. In addition, quantitative erosion rate data gives coastal managers the advantage of making proactive rather than reactive policy decisions. Experience has shown that reactive or inappropriate decisions in the coastal zone can have deleterious economic, social and environmental consequences.

Shoreline erosion in Puerto Rico, both natural and human-induced, is relatively well documented (Turner, 1956; Morelock, 1978; 1984; Thieler and Danforth, 1993; Bush *et al.*, in press). The response to shoreline erosion in Puerto Rico has been crisis-based, non-coordinated engineering of the coast. Typical responses have been, in various places, construction of groins, seawalls and revetments and building of artificial dunes. These structures have had a significant impact on local erosion rates. This report documents historical shoreline changes along a small portion of the Puerto Rico coast and interprets the environmental significance of the various mechanisms responsible for these changes.

STUDY AREA

Puerto Rico is the smallest and easternmost of the Greater Antilles islands. The island is about 160 km long and 50 km wide (Fig. 1). Rincón is located on the west coast (Fig. 2).

The study area at Rincón extends from Punta Higüero to Punta Cadena. These rocky headlands are extensions of the central mountain belt that runs the width of Puerto Rico, and form the boundaries of the Rincón-Córcega littoral cell (Morelock, 1987). The shoreline between the headlands is a low-lying alluvial plain with a sandy beach (Fig. 3). From Punta Higüero to Punta Ensenada, however, abundant outcrops of beachrock, eolianite and metasedimentary rocks are present along the shoreline (Fig. 4).

The wave climate on the northwestern coast of Puerto Rico is strongly seasonal. The largest waves occur during the winter months. In fact, the portion of the study area north of Punta Ensenada (see Fig. 2) is the location of a number of world-famous surfing breaks (Pilkey, 1976; The Surf Report, 1982). The longshore gradient in wave energy during large swell events is quite strong. When breaking wave heights north of Punta Ensenada are larger than 4-5 m, the area south of Córcega is usually subject to only a small swell of about 1 m. This is due in part to the sheltering effect of nearshore reefs in the study area, and the slightly broader shelf on which the reefs are located. During the summer, however, the seas are nearly flat along the entire study area, except during the passage of atmospheric tropical waves. The study area is a microtidal environment (tidal range $\approx$ 0.2 m); tides are semidiurnal.

The beaches within the study area are composed primarily of biogenic shelf carbonates and river-derived terrigenous material (Morelock, 1987). The primary sources of new sediment to the beach system are biological production and bioerosion of nearshore reefs and erosion of both modern and relict alluvial deposits along the shoreline (Morelock, 1987). The net direction of longshore drift is to the south.

Morelock (1987) described the western coast of Puerto Rico as compartmentalized, with little to no communication between adjacent littoral cells. The insular shelf between Punta Higüero and Punta Cadena (the Rincón-Córcega littoral cell) is generally less than a few hundred meters

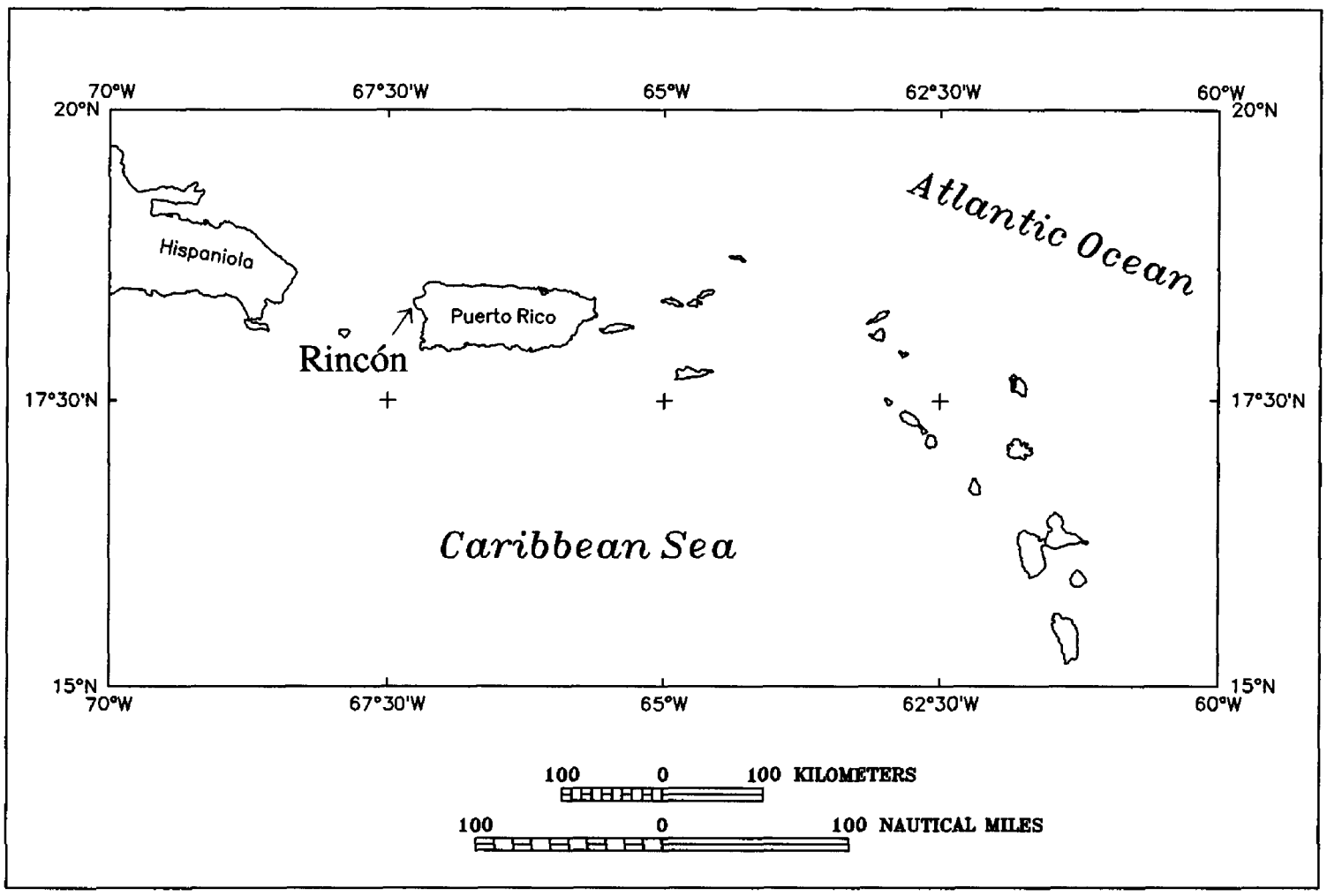
70°W
67°30'W
65°W
62°30'W
60°W
20°N
17°30'N
15°N
Hispaniola
Puerto Rico
Rincón
Atlantic Ocean
Caribbean Sea
100 0 100 KILOMETERS
100 0 100 NAUTICAL MILES

Figure 1

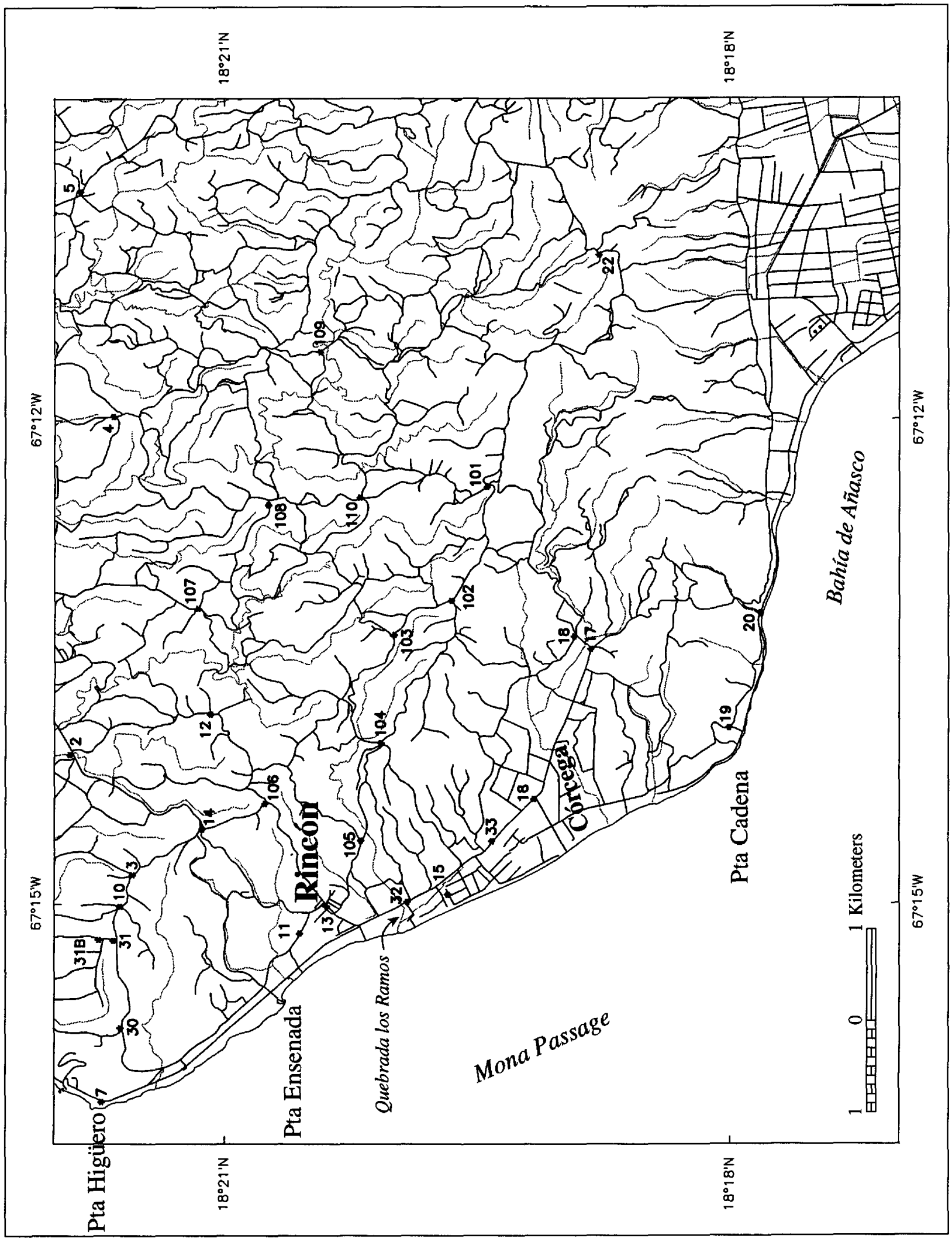
67°12'W
18°21'N
18°18'N
67°15'W
Bahía de Añasco
Rincón
Pta Higüero
Pta Ensenada
Quebrada los Ramos
Mona Passage
Córcega
Pta Cadena
1 Kilometers
0
1
2
3
4
5
7
10
11
12
13
14
15
17
18
19
20
22
30
31
31B
32
33
101
102
103
104
105
106
107
108
109
110

Figure 2

Figure 3

Figure 4

wide. This situation further limits sediment transport between littoral cells; some sand is probably lost off the shelf into deeper water.

North of Punta Ensenada, the shoreline is mostly undeveloped, with small farm plots bordering the back of the beach. At Punta Ensenada, a small marina facility was built in 1983 (Fig. 5). The marina entrance is maintained by two parallel breakwaters. South of the marina, shoreline development consists primarily of single family homes and small tourist hotels. For the most part, the buildings are set back about 10 m from the shoreline. In some locations, however, persistent shoreline erosion has reached the beachfront row of buildings. This has resulted in the proliferation of seawalls and revetments of varying size and quality of construction: some are built of large quarry stone, while others are built primarily of construction rubble (Fig. 6). South of the Córcega community (see Fig. 2), the shoreline is again backed by small farm plots. Near Punta Cadena, houses are set well back from the shoreline atop the low hills of the Cerros de San Francisco.

METHODS

The methods used for this study can be divided into three steps: 1) obtaining shoreline positions from the historical aerial photography; 2) obtaining shoreline positions using field GPS surveys; and 3) computation of shoreline rates-of-change (erosion rates). These steps are described below.

Air Photos

Seven sets of near-vertical, overlapping aerial photographs were used to obtain historical shoreline positions. The data include sets of photography from the following years: 1950, 1963, 1971, 1974, 1977, 1987 and 1989. All have a nominal scale of 1:20,000 except the 1950 photos, which are at 1:15,000. All photos, except the 1987 set which used natural color film, were taken in black and white. All of the photographic surveys were flown during the winter months.

The air photo-derived shoreline data were produced using the Digital Shoreline Mapping System (DSMS), a computer-based system which produces digital shoreline position data from historical maps, charts and aerial photographs. A complete description of DSMS execution is furnished by Danforth and Thieler (1992b). Further technical background on the techniques described below is provided by Thieler and Danforth (1994a and 1994b).

A ground control network for the air photos was developed by identifying a number of common features on most or all of the photograph sets. Stable reference features such as buildings and road intersections were identified and their approximate locations marked on a U.S. Geological Survey (USGS) 7.5-minute topographic map. The points were then precisely located in the field and a more specific, stable target (*e.g.*, a building corner, sidewalk, *etc.*) identifiable on the photographs was surveyed using a differential Global Positioning System (GPS) receiver. The points used in this study are accurate horizontally within 3 m and vertically to within about 6 m. Ground control point locations are shown as numbered points in Figure 2. Once the basic control network was established, a suite of pass points (common points appearing on two or more photos for which precise geographic information is unknown) was identified to provide further relative control for the photos within each time series (see Thieler and Danforth, 1994a, their Figure 4 and discussion). To provide a very "tight" control network and permit greater photogrammetric accuracy, the photo sets for each date included frames that were well inland from the shoreline.

The air photos were digitized using a 12*x* lighted magnifying loupe to aid in identification of the fiducial reference marks around the photo border, ground control points, pass points, and the shoreline. The wet/dry line on the beach, the reference feature used in the field surveys described below, was used to delineate the shoreline in each photo. The wet/dry line is the most frequently used shoreline for digitizing because it is easily identified by the tonal difference

Figure 5

Figure 6

between wet and dry sand (Dolan *et al.*, 1980; Crowell *et al.*, 1991). Where available, camera system calibration data were used in the DSMS to correct the photographs for film distortion and assess the magnitude of lens distortion.

The National Ocean Service's General Integrated Analytical Triangulation (*GIANT*) aerotriangulation program, which forms a part of the DSMS, was used to solve simultaneously for the camera position and angular orientation parameters for the air photos. *GIANT* was also used to remove atmospheric refraction effects from the aerotriangulation solution. Statistical output from *GIANT* indicated an accuracy of ±4 m for the air photo-derived shoreline locations.

The camera parameters for each photo were used to compute a single-ray intersection solution for the digitized shoreline points using the method described by Thieler and Danforth (1994a). A geographic coordinate system based on the WGS84 ellipsoid was used in shoreline position calculations for consistency with the GPS control point surveys and the field shoreline surveys described below. The output shoreline position data files for each photo were imported into separate overlays (one for each year of photography) in MapInfo™, a Macintosh®-based Geographic Information System (GIS), and joined to adjacent photo data to form a continuous shoreline.

GPS Field Surveys

Two field surveys of wet/dry shoreline position were conducted on 06 February and 24 August 1994. These surveys utilized a backpack-mounted GPS receiver logging positions at 5-second intervals as the backpacker walked along the wet/dry line (Fig. 7). The data were differentially corrected in real-time in the field. Further post-processing yielded a positioning accuracy of 2-3 m. The GPS data were imported directly into the GIS for display with the shorelines obtained from the photographs.

Computation of Erosion Rates

In the GIS, a measurement baseline was established landward of the nine shorelines by drawing a series of connected, straight line segments parallel to the general shoreline trend from Punta Higüero to Punta Cadena. The shoreline and baseline data were used to calculate shoreline rates-of-change at 100 m intervals (transects) along the baseline using the Digital Shoreline Analysis System (Danforth and Thieler, 1992a).

The output rate-of-change data include the four rate-of-change statistics reviewed by Dolan *et al.* (1991). These methods include the end-point rate (*epr*), linear regression (*lr*), jackknifing (*jk*), and average of rates (*aor*) (Fig. 8). The *epr* is calculated by dividing the total distance of shoreline movement by the time elapsed between the earliest and latest measurements (*i.e.*, the oldest and the most recent shoreline positions). For each transect, the *lr* rate is determined by fitting a least squares regression line to a plot of the shoreline locations (as measured by their distance from the baseline) versus time. The *lr* rate is the slope of the line. The *jk* is determined by performing iteratively a linear regression for all possible combinations of shoreline positions for each transect, omitting one point in each iteration. The slopes of each regression line are then averaged to obtain the *jk* rate.

Based on an analysis of the shoreline trends described below, the *aor* was chosen as the most appropriate statistic to describe the rate of shoreline change in the study area. The *aor* method was developed by Foster and Savage (1989) for use along the Florida coastline. This method involves calculating separate end-point rates for all combinations of shoreline locations when more than two are present at a particular transect. All end-point rates for a transect are then averaged to

Figure 7

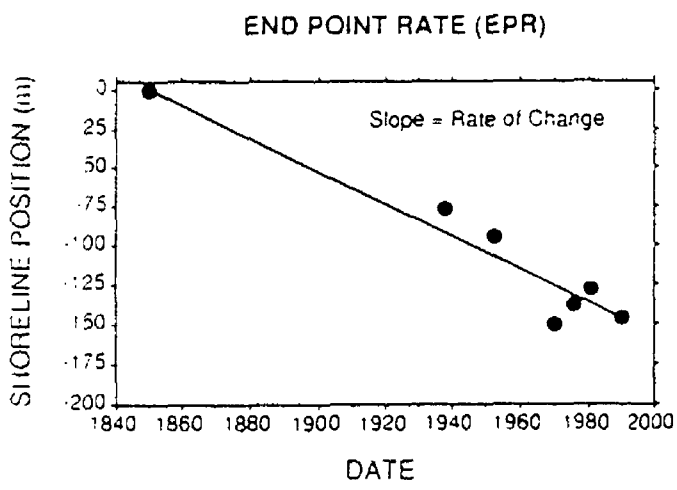
END POINT RATE (EPR)
SHORELINE POSITION (m)
0
-25
-50
-75
-100
-125
-150
-175
-200
1840 1860 1880 1900 1920 1940 1960 1980 2000
DATE
Slope = Rate of Change

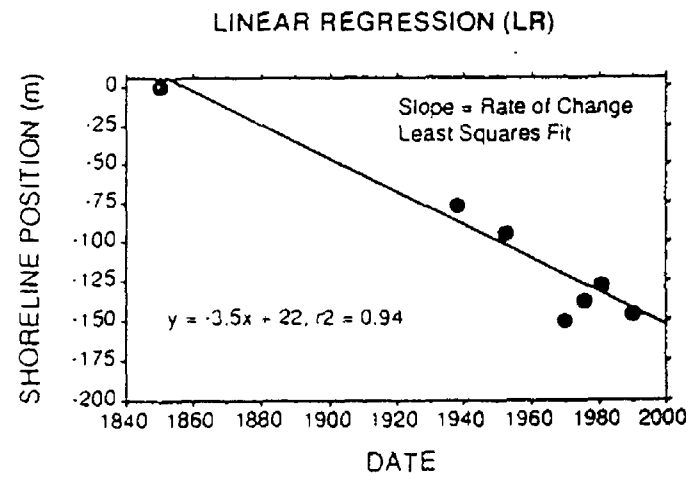
LINEAR REGRESSION (LR)
SHORELINE POSITION (m)
0
-25
-50
-75
-100
-125
-150
-175
-200
1840 1860 1880 1900 1920 1940 1960 1980 2000
DATE
Slope = Rate of Change
Least Squares Fit
y = -3.5x + 22, r2 = 0.94

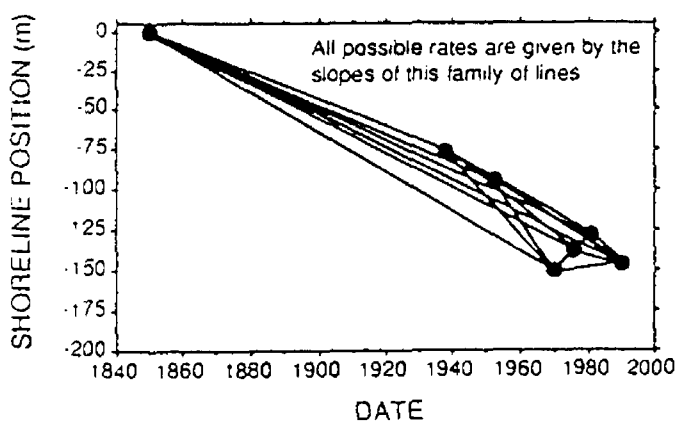
AVERAGE OF RATES (AOR)
SHORELINE POSITION (m)
0
-25
-50
-75
-100
-125
-150
-175
-200
1840 1860 1880 1900 1920 1940 1960 1980 2000
DATE
All possible rates are given by the
slopes of this family of lines

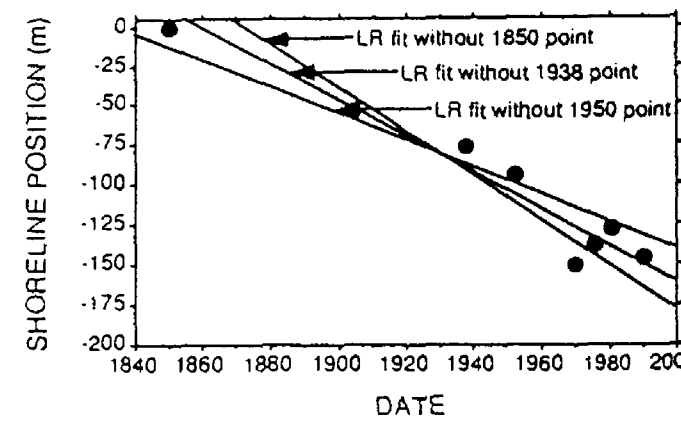
JACKKNIFE (JK)
SHORELINE POSITION (m)
0
-25
-50
-75
-100
-125
-150
-175
-200
1840 1860 1880 1900 1920 1940 1960 1980 2000
DATE
LR fit without 1850 point
LR fit without 1938 point
LR fit without 1950 point

Figure 8

obtain the *aor* rate. Foster and Savage (1989) developed an equation to evaluate whether any given *epr* for a transect meets a minimum time criterion, T_{min}:

$$T_{min} = \frac{\sqrt{(E_1)^2 + (E_2)^2}}{R_1} \quad (1)$$

where E_1 and E_2 are the measurement errors in the first and second shoreline point, and R_1 is the *epr* of the longest time span for the transect (Dolan *et al.*, 1991). For this study, E_1 and E_2 are both considered to be 4.0 m. This value was determined based on analysis of the photogrammetric transformations and the accuracy of the GPS field surveys.

The *aor* method also provides a measure of the standard deviation and variance of the data. If only two shoreline points are present at a transect, and the T_{min} requirement is met, then the *aor* is the same as the *epr*, with a standard deviation and variance of zero. If all combinations of end-point rates fail to meet the T_{min} requirement, then the *aor* is undefined for that transect. In this case, the *epr* value is used to represent the *aor*.

Dolan *et al.* (1991) describe several advantages to using the *aor* method relative to other rate-of-change statistics. First, the data must meet the minimum time criterion, T_{min}. Thus, only the "good" data are used. In other words, *epr* combinations for a transect that fail to meet the T_{min} requirement are not used in the *aor* calculation. Second, the *aor* method is sensitive to large shifts in trends of shoreline behavior and filters short-term variations in shoreline behavior. Third, the method is useful for dealing with data that are clustered or irregularly spaced in the temporal domain. For example, the present data set includes shoreline positions spaced relatively widely in time prior to 1971 (1950, 1963, and 1971), three shoreline positions in the 1970's (1971, 1974, and 1977), and four later shoreline positions (1987, 1989, February and August 1994).

The primary disadvantages to the *aor* method cited by Dolan *et al.* (1991) are the lack of a computational norm for calculating T_{min} and the sensitivity of the results to the assumed E_1 and E_2 measurement errors. These shortcomings are not viewed as strongly detrimental to the analysis of this data set. As discussed below, the *aor* results are generally consistent with the results obtained using the other three methods.

RESULTS

Shoreline rates-of-change were calculated at 89 transects. Table 1 shows the four rate-of-change statistics calculated for each transect in the study area. In this study, the resolution of long-term, end-point rates is approximately 0.2 m/yr. That is, the inherent errors in the shoreline position (about 4 m for each shoreline; 8 m total when comparing two shorelines), coupled with the time span of the study (44 years), yield a "signal to noise" ratio of 0.18 m/yr. For simplicity, this number is rounded to 0.2 m/yr. Thus, rates-of-change less than ±0.2 m/yr for a given transect are considered undetectable.

The transect locations and rate-of-change histograms are shown in Figure 9. Based on the rate-of-change data (hereafter, "erosion rate" since that is the dominant trend), the study area can be divided into four reaches (Fig. 9).

Table 2 provides a summary of the data for each shoreline reach. Over the period 1950-1994, erosion is the predominant trend in the study area, averaging 0.35 m/yr. The maximum erosion rate, at transect 36, is 2.34 m/yr, while the minimum value indicates 0.42 m/yr of accretion at transect 27 (Fig. 9). When divided into shoreline reaches, however, the spatial distribution of erosion rates is more readily visible.

Table 1. Shoreline rates-of-change for the 89 transects between Punta Higüero and Punta Cadena shown on Plate 1 and Figure 9.

Transect	*epr* (m/yr)	*aor* (m/yr)	σ *aor*	s^2 *aor*	*lr* (m/yr)	*jk* (m/yr)	Transect	*epr* (m/yr)	*aor* (m/yr)	σ *aor*	s^2 *aor*	*lr* (m/yr)	*jk* (m/yr)
1	-0.10	*	*	*	-0.04	-0.05	46	-0.89	-0.82	0.80	0.63	-0.65	-0.64
2	-0.25	-0.04	0.14	0.02	-0.11	-0.10	47	-0.73	-0.48	0.48	0.23	-0.49	-0.49
3	0.02	*	*	*	0.03	0.03	48	-0.40	-0.30	0.53	0.28	-0.26	-0.27
4	-0.14	-0.14	0.00	0.00	-0.01	-0.01	49	-0.35	-0.23	0.37	0.14	-0.15	-0.15
5	0.03	*	*	*	0.01	0.01	50	-0.63	-0.16	0.46	0.21	-0.25	-0.24
6	-0.11	*	*	*	-0.14	-0.14	51	-0.67	-0.23	0.42	0.18	-0.31	-0.30
7	-0.22	-0.23	0.23	0.06	-0.22	-0.23	52	-0.60	-0.22	0.42	0.17	-0.28	-0.27
8	-0.07	*	*	*	-0.01	-0.01	53	-0.63	-0.23	0.43	0.18	-0.32	-0.31
9	0.09	*	*	*	0.07	0.06	54	-0.63	-0.32	0.36	0.13	-0.40	-0.39
10	0.10	*	*	*	0.05	0.04	55	-0.50	-0.33	0.36	0.13	-0.35	-0.34
11	-0.01	*	*	*	-0.07	-0.09	56	-0.52	-0.35	0.40	0.16	-0.36	-0.35
12	0.10	*	*	*	0.06	0.05	57	-0.60	-0.33	0.53	0.28	-0.39	-0.38
13	-0.04	*	*	*	-0.02	-0.03	58	-0.64	-0.28	0.63	0.40	-0.41	-0.39
14	0.19	0.19	0.14	0.02	0.18	0.18	59	-0.65	-0.29	0.56	0.32	-0.38	-0.37
15	0.20	0.13	0.07	0.00	0.10	0.09	60	-0.65	-0.28	0.52	0.27	-0.37	-0.35
16	0.28	0.18	0.50	0.25	0.11	0.09	61	-0.94	-0.64	0.84	0.71	-0.55	-0.54
17	0.42	0.19	0.43	0.18	0.25	0.23	62	-0.89	-0.64	0.69	0.47	-0.57	-0.56
18	0.02	*	*	*	-0.05	-0.05	63	-0.23	-0.26	0.34	0.11	-0.30	-0.31
19	-0.01	*	*	*	-0.10	-0.11	64	-0.26	-0.33	0.34	0.11	-0.32	-0.33
20	-0.10	*	*	*	-0.19	-0.20	65	-0.06	*	*	*	-0.19	-0.21
21	-0.16	-0.19	0.07	0.01	-0.28	-0.29	66	-0.10	*	*	*	-0.22	-0.23
22	-0.07	*	*	*	-0.16	-0.17	67	-0.11	*	*	*	-0.23	-0.24
23	0.16	0.11	0.04	0.00	0.01	0.00	68	-0.09	*	*	*	-0.18	-0.19
24	-0.21	-0.22	0.05	0.00	-0.24	-0.24	69	-0.09	*	*	*	-0.17	-0.17
25	-0.09	*	*	*	-0.18	-0.19	70	-0.22	-0.35	0.13	0.02	-0.24	-0.24
26	0.05	*	*	*	0.03	0.02	71	-0.31	-0.18	0.34	0.11	-0.21	-0.20
27	0.58	0.42	0.63	0.40	0.41	0.40	72	-0.11	*	*	*	-0.02	-0.02
28	0.27	0.16	0.23	0.05	0.20	0.19	73	-0.13	-0.09	0.04	0.00	-0.08	-0.08
29	-0.03	*	*	*	-0.01	-0.01	74	0.00	*	*	*	0.07	0.08
30	-0.09	*	*	*	-0.03	-0.04	75	-0.04	*	*	*	0.03	0.04
31	0.09	*	*	*	0.00	-0.01	76	-0.20	-0.07	0.11	0.01	-0.06	-0.05
32	-0.58	-0.99	0.81	0.65	-0.87	-0.88	77	-0.47	-0.31	0.34	0.12	-0.33	-0.32
33	-1.01	-1.33	1.38	1.91	-1.23	-1.24	78	-0.16	-0.16	0.04	0.00	-0.19	-0.19
34	-1.43	-1.46	1.21	1.45	-1.50	-1.52	79	-0.07	*	*	*	-0.16	-0.16
35	-1.68	-1.93	1.48	2.19	-2.00	-2.02	80	-0.27	-0.22	0.18	0.03	-0.24	-0.24
36	-1.84	-2.34	1.71	2.91	-2.23	-2.26	81	-0.39	-0.41	0.34	0.12	-0.37	-0.37
37	-1.65	-2.19	1.83	3.35	-1.89	-1.92	82	-0.14	*	*	*	-0.17	-0.19
38	-1.52	-2.19	2.57	6.60	-1.60	-1.64	83	-0.10	*	*	*	-0.04	-0.03
39	-1.55	-2.14	2.46	6.05	-1.91	-1.95	84	-0.40	-0.37	0.30	0.09	-0.33	-0.31
40	-1.08	-1.00	0.89	0.79	-0.92	-0.92	85	-0.01	*	*	*	0.04	0.05
41	-1.40	-1.09	0.78	0.60	-1.06	-1.04	86	0.01	*	*	*	0.09	0.11
42	-1.39	-1.17	0.87	0.75	-1.08	-1.07	87	-0.01	*	*	*	0.01	0.01
43	-1.43	-1.45	0.93	0.87	-1.31	-1.30	88	0.19	0.19	0.00	0.00	0.23	0.23
44	-1.29	-1.54	1.31	1.72	-1.33	-1.33	89	0.04	*	*	*	0.03	0.02
45	-1.16	-1.12	1.42	2.01	-1.02	-1.02							

Notes: Negative rate values indicate erosion. Histograms for the average of rates (*aor*) are shown in Figure 9. Dolan *et al.* (1991) provide a complete discussion of the utility of each rate calculation.

(*epr* = end-point rate; *aor* = average of rates; σ *aor* = standard deviation of average of rates; s^2 *aor* = variance of average of rates; *lr* = linear regression rate; *jk* = jackknife rate; * = data fail to meet the minimum change required to use this method; in this case, the *aor* value shown in Figure 9 defaults to the *epr*.)

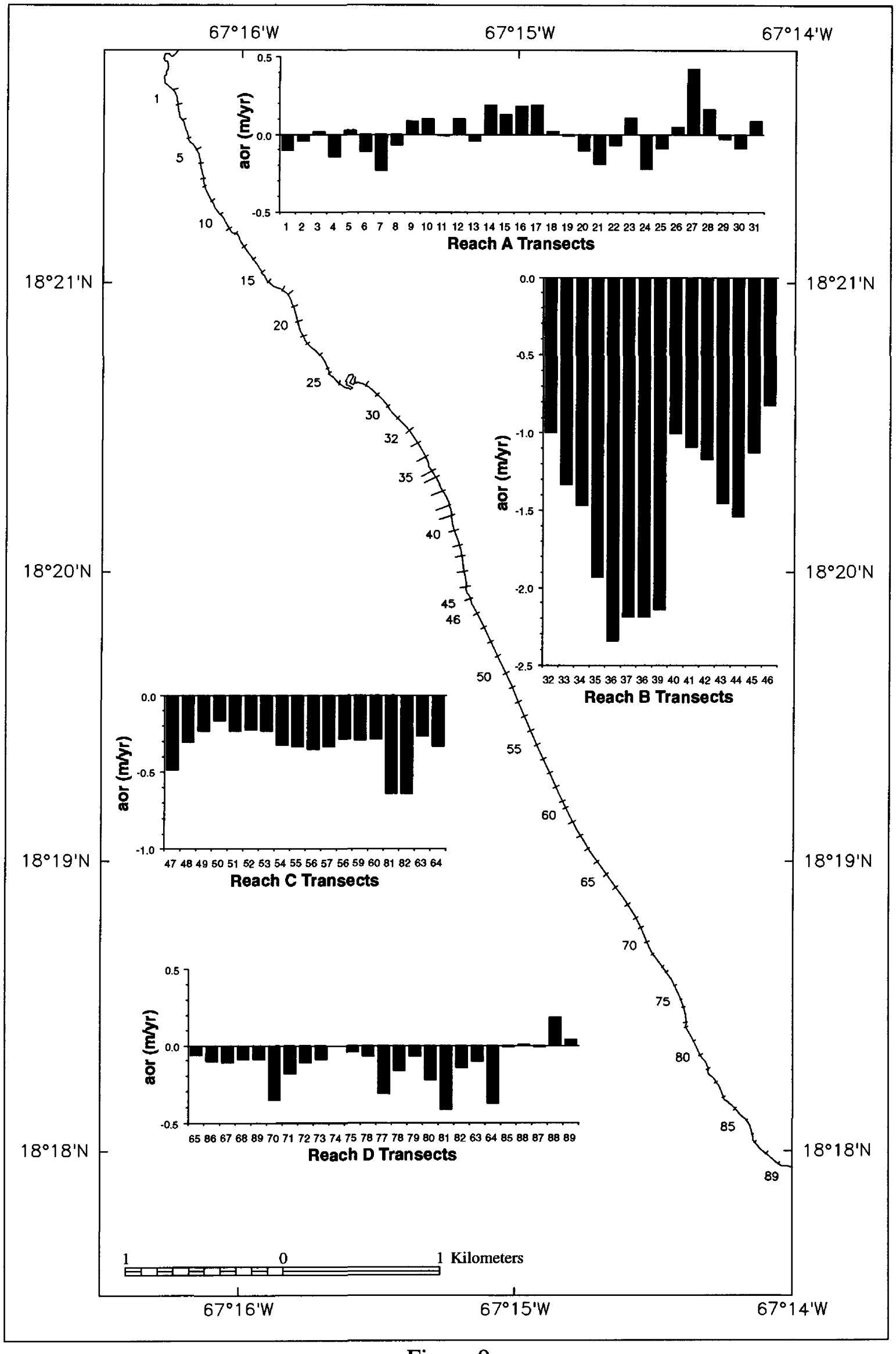
67°16'W
67°15'W
67°14'W
18°21'N
18°20'N
18°19'N
18°18'N
aor (m/yr)
Reach A Transects
Reach B Transects
Reach C Transects
Reach D Transects
1 0 1 Kilometers

Figure 9

Table 2. Erosion rate summary for the four shoreline reaches shown in Figure 9 over the period 1950-1994.

Reach	Category	*epr* (m/yr)	*aor* (m/yr)	*lr* (m/yr)	*jk* (m/yr)
All	Average	-0.37	-0.35	-0.34	-0.34
	Std. Dev.	0.53	0.59	0.53	0.54
	Variance	0.28	0.35	0.28	0.29
	Max. Accretion	0.58	0.42	0.41	0.40
	Max. Erosion	-1.84	-2.34	-2.23	-2.26
Reach A	Average	0.03	0.01	-0.01	-0.02
	Std. Dev.	0.19	0.14	0.15	0.15
	Variance	0.03	0.02	0.02	0.02
	Max. Accretion	0.58	0.42	0.41	0.40
	Max. Erosion	-0.25	-0.23	-0.28	-0.29
Reach B	Average	-1.33	-1.52	-1.37	-1.38
	Std. Dev.	0.33	0.51	0.47	0.48
	Variance	0.11	0.26	0.22	0.23
	Min. Erosion	-0.58	-0.82	-0.65	-0.64
	Max. Erosion	-1.84	-2.34	-2.23	-2.26
Reach C	Average	-0.58	-0.33	-0.36	-0.35
	Std. Dev.	0.19	0.13	0.10	0.10
	Variance	0.04	0.02	0.01	0.01
	Min. Erosion	-0.23	-0.16	-0.15	-0.15
	Max. Erosion	-0.94	-0.64	-0.57	-0.56
Reach D	Average	-0.13	-0.11	-0.12	-0.12
	Std. Dev.	0.15	0.14	0.15	0.15
	Variance	0.02	0.02	0.02	0.02
	Max. Accretion	0.19	0.19	0.23	0.23
	Max. Erosion	-0.47	-0.41	-0.37	-0.37

Notes: Negative rate values indicate erosion. Abbreviations are the same as in Table 1.

Table 3. Erosion rate summary for the four shoreline reaches, comparing the periods 1950-1977 and 1987-1994.

Reach	Category	*aor* 1950-1977 (m/yr)	*aor* 1987-1994 (m/yr)
All	Average	-0.13	-0.96
	Std. Dev.	0.63	1.51
Reach A	Average	0.23	-0.36
	Std. Dev.	0.31	0.85
Reach B	Average	-0.56	-3.12
	Std. Dev.	1.15	1.94
Reach C	Average	-0.40	-0.98
	Std. Dev.	0.47	0.57
Reach D	Average	-0.12	-0.03
	Std. Dev.	0.30	0.56

Notes: Negative rate values indicate erosion.
Abbreviations are the same as in Table 1.

The spatial position of the nine shorelines over time shown in Plate 1 indicate a profound change in the trend of shoreline behavior after 1977. Table 3 (above) shows the average erosion rates for the four shoreline reaches for two periods, 1950-1977 and 1987-1994. This temporal partitioning of the data shows clearly that a significant change in trend took place between 1977-1987. For the entire study area, the rate of erosion increased by a factor of seven (Table 3). Except for Reach D, which has rates-of-change below the 0.2 m/yr resolution of the data, there was a shift toward increasing erosion within each reach.

Reach A

In general, the shoreline in Reach A appears to be fairly stable. Both the *epr* and *aor* indicate very minor accretion over the 44-year study period, while the *lr* and *jk* rates indicate very minor erosion. All of these rates, however, are below the 0.2 m/yr resolution of the data set.

The change in trend between 1950-1977 and 1987-1994 (Table 3) appears as a detectable shift from moderate accretion (0.23 m/yr) to moderate erosion (0.36 m/yr).

Reach B

The shoreline in this reach has the highest erosion rates in the study area. Nearly all rates are greater than 1.0 m/yr, and several hundred meters of shoreline are eroding at over 2.0 m/yr. Over the period 1950-1994, the lowest erosion rate in this reach is 0.58 m/yr.

This reach has also been most affected by the change in trend that occurred between 1977-1987. The data shown in Table 3 indicate that the trend changed from moderate erosion (0.56 m/yr) to a severe erosion rate of more than 3.0 m/yr. In fact, several transects have erosion rates >5.0 m/yr; the highest is 6.34 m/yr. In comparison to shoreline change data for Puerto Rico presented by Thieler and Danforth (1993), this is the most rapidly eroding shoreline on the entire island.

Reach C

Over the last 44 years, this reach has been eroding at about 0.33 m/yr (Table 1). The erosion rates in this reach are lower than in Reach B, but the trend is insistent; the standard deviation is well below the mean.

The erosion rate between 1987-1994 (0.98 m/yr) is more than twice the rate over the period 1950-1977 (0.40 m/yr). The interesting feature in shoreline behavior here, however, occurs in the middle of the reach. Figure 10 shows a histogram that compares the end-point erosion rate over the periods 1950-1977 and 1987-1994. North of Transect 56, the erosion rate has increased dramatically in the past seven years. Farther south, however, the erosion rate has actually *decreased*. (Note that here we use the end-point [*epr*] rate, rather than the *aor*. This is due to the increasing sensitivity of the *aor* to the E_1 and E_2 errors described above. Most of the transects in this reach analyzed with this temporal division default to the *epr* due to insufficient time spans for obtaining a useful *aor* statistic.)

Reach D

All the rate-of-change values for Reach D are below the 0.2 m/yr resolution of the data. However, field evidence and local observations indicate that the erosion rate in Reach D is low, and may in fact be close to the 0.11 m/yr value shown in Table 2. The data in Table 3 also indicate a very minor reduction in the erosion rate between the two periods 1950-1977 and 1987-1994.

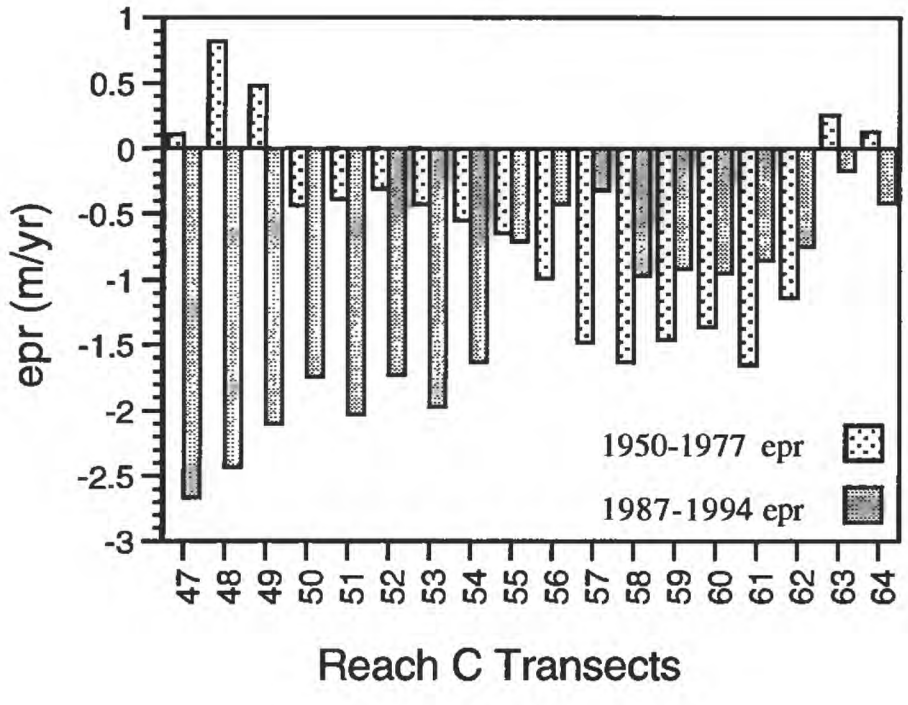
epr (m/yr)
1
0.5
0
-0.5
-1
-1.5
-2
-2.5
-3
47
48
49
50
51
52
53
54
55
56
57
58
59
60
61
62
63
64
1950-1977 epr
1987-1994 epr
Reach C Transects

Figure 10

DISCUSSION

There are several factors that help explain the spatial and temporal variability in shoreline changes in the study area. These include geomorphologic factors, as well as human-induced perturbations to the system. The trends in each of the four shoreline reaches and their underlying causes are discussed below.

Reach A

The shoreline in Reach A has the highest wave energy in the study area. Nonetheless, the long-term (44-year) trend indicates a stable shoreline (Table 2). This relative stability is due in part to the rocky nature of the shoreline.

As shown in Figure 4, portions of the shoreline are composed of Recent beachrock deposits. In addition, there are exposures of Pleistocene eolianite (Kaye, 1959) extending northward from Punta Ensenada for several hundred meters. Near Punta Higüero, the metasedimentary rocks of the adjacent mountains either crop out or form a shallow, terrace-like subcrop along the shoreline.

Along most of this reach, the shoreline is not composed of a purely sandy substrate. In fact, the beach amounts to a small prism of sand that migrates back and forth across the slowly eroding surface of the rock units, with a net landward trend.

Reach B

In contrast to Reach A, the shoreline in this reach is composed almost entirely of unconsolidated, sandy, alluvial sediments. Figure 11 shows the well-developed scarp that is present along the southern part of the reach. Given the relatively low rate of sediment supply from the rocky coast in Reach A, shoreline erosion probably contributes the majority of the new sediment to the beach system here.

Reach B is also the site of the largest human alterations to the coastal system in the study area. Specifically, it appears that the marina built in 1983 is both directly and indirectly responsible for most of the increased erosion. The marina has probably had several impacts on this and adjacent downdrift reaches. It may be that the seaward breakwater (Fig. 5) is preventing the longshore movement of sand around Punta Ensenada and into Reach B. This is due to the change in shoreline configuration caused by the breakwater. A gently curving, shallow spit of sand underlain by a rock unit (eolianite?) was present prior to the marina's construction. This setting was changed by the emplacement of a large rock structure that extends out into fairly deep water. It is likely that the breakwater is causing an offshore deflection of longshore drift into deeper water where it is not returned to the beach (*i.e.*, the sediment is effectively removed from the beach system). The shore-normal, channeled nature of the nearshore reef system may enhance this effect. As discussed above, the proximity of the shelf break to this area probably results in significant losses of sediment offshore.

There is also evidence that the breakwater has changed the pattern of nearshore sand deposition: a deposit of sand is accumulating at the marina entrance. The rate of sediment accumulation in front of the marina is sufficiently rapid to require periodic dredging. Local observers indicate that the dredged material typically is removed illegally and used for building construction.

The erosion rate in Reach B shows the most profound increase of all reaches between the two periods 1950-1977 and 1987-1994: the average rate increased from 0.56 m/yr to 3.12 m/yr. Where this erosion has threatened beachfront development, a variety of gabion walls, revetments

Figure 11

and seawalls have been built (see Fig. 6). This response is probably reducing the availability of new sediment to the system. The following example illustrates this point.

About one kilometer of shoreline along Reach B (Transects 36-46) has been eroding at nearly 4.0 m/yr since 1987. Much of the shoreline here is formed by a 2-meter high scarp in unconsolidated alluvial deposits (see Fig. 11). Thus, the erosion rate in this section represents a volume removal of approximately 8 m^3/m/yr, or about 8000 m^3/yr for this one kilometer of shoreline alone. Relative to the size of the coastal compartment formed by Reaches B-D (about 6 km), this volume is probably a significant portion of the entire sediment budget. Reducing this sediment supply by constructing seawalls may well result in a dramatic increase in erosion on downdrift beaches in Reaches C and D.

Reach C

For the area south of Transect 56, the decrease in erosion rate over the period 1987-1994 is probably the result of increased sediment supply from the eroding alluvial sediments updrift in the southern part of Reach B and the northern part of Reach C. It appears that beaches downdrift of the zone of maximum erosion in Reach B are benefiting from an increased sand supply. As shown in Figure 12, the beach here is quite "healthy," although it is eroding over the long-term at nearly 1.0 m/yr.

Reach D

Like the southern portion of Reach C, this reach appears to be benefiting from the increased sediment supply from erosion in Reach B. The data in Table 3 indicate a slightly reduced erosion rate over the past seven years, although the actual rates-of-change here are so low as to be undetectable.

The generally low erosion rates are probably also due in part to the increasingly rocky nature of the shoreline here. Like Reach A to the north, in many places the beach is a small prism of sand that migrates across a rocky substrate.

Figure 12

CONCLUSIONS

The shoreline of the northwestern coast of Puerto Rico, from Punta Higüero to Punta Cadena, has been eroding over the last 44 years. The spatial distribution of erosion rates permits this shoreline to be divided into four distinct reaches (A-D) from north to south. The study area has also experienced a dramatic increase in erosion rates over the past seven years.

Reach A has had an essentially stable shoreline over the period 1950-1994. This is due in part to the rocky nature of the shoreline. Beachrock, eolianite and metasedimentary rocks form a low-relief, shallow terrace on which the beach lies. The beach here amounts to a small prism of sand that probably migrates seasonally back and forth over this surface. Since 1987, however, the net trend has changed from accretion to erosion.

The shoreline in Reach B is eroding most rapidly, at a rate just over 1.5 m/yr for the past 44 years. Over the past seven years, however, approximately one kilometer of shoreline has been eroding at nearly 4.0 m/yr into a two-meter high, unconsolidated alluvial bluff. This erosion probably represents a significant portion of the sediment supply to the southern six kilometers of the study area.

In Reach C, the rate of erosion is fairly low over the past 44 years (0.33 m/yr). In general, the northern portion of the reach is eroding more rapidly than the southern portion, but the beaches still appear healthy. Since 1987, the erosion rate in southern portion of this reach has actually decreased. The lower rate of erosion is probably due to the increase in sediment supply from the rapidly eroding shoreline farther updrift.

The shoreline in Reach D appears to be fairly stable. The long-term rate of erosion is within the resolution of the methods used in this study. There has been no detectable change in trend over the past seven years. Field evidence, however, indicates a very low long-term erosion rate.

The 1983 construction of a marina, including two breakwaters/jetties at its entrance, appears to be responsible for a dramatic increase in erosion rates. A one-kilometer stretch of shoreline south of the marina entrance is presently eroding at nearly 4.0 m/yr. This is the highest erosion rate in Puerto Rico.

The marina is probably having two effects on nearshore sedimentation. First, the seaward breakwater has changed the shoreline configuration such that longshore drift is likely being deflected into deeper water, and perhaps over the shelf break. Second, the breakwater may also have changed nearshore wave refraction patterns. This is evidenced by increased sedimentation at the marina entrance.

The increased shoreline erosion south of the marina probably represents the most significant source of new sediment to this littoral system. In fact, the rate of erosion on downdrift beaches has actually decreased since the marina was built. This is likely because of an increase in sediment supply due to the marina-induced, accelerated erosion. The response to increased erosion has been the construction of seawalls and revetments. This action will reduce the sediment supply, and cause an increase in erosion rates on downdrift beaches. The present trend of seawall and revetment construction suggests that the problem will only worsen over time.

ACKNOWLEDGMENTS

This project was supported by the San Juan Field Office of the U.S. Geological Survey, Branch of Atlantic Marine Geology as part of an ongoing investigation of beach dynamics in the Rincón area. Rafael Rodríguez is thanked for helpful discussions and field support. Barry Irwin

provided technical assistance with the GPS surveys. Juan Trías assisted in the office and in the field.

REFERENCES

Bush, D.M., Webb, R. M. T., Hyman, L., González-Liboy, J., and Neal, W. J., in press. *Living with the Puerto Rico Shore*: Durham, North Carolina, Duke University Press.

Crowell, M., Leatherman, S. P., and Buckley, M. K., 1991. Historical shoreline change: Error analysis and mapping accuracy. *Journal of Coastal Research*, v. 7, no. 3, p. 839-852.

Danforth, W. W., and Thieler, E. R., 1992a. *Digital Shoreline Analysis System (DSAS) User's Guide, Version 1.0*. Reston, Virginia: U.S. Geological Survey Open-File Report No. 92-355, 42 p.

Danforth, W. W., and Thieler, E. R., 1992b. *Digital Shoreline Mapping System (DSMS) User's Guide, Version 1.0*. Reston, Virginia: U.S. Geological Survey Open-File Report 92-240, 33 p.

Dolan, R., Fenster, M. S., and Holme, S. J., 1991. Temporal analysis of shoreline recession and accretion. *Journal of Coastal Research*, v. 7, no. 3, p. 723-744.

Dolan, R., Hayden, B. P., May, P., and May, S., 1980. The reliability of shoreline change measurements from aerial photographs: *Shore and Beach*, v. 48, no. 4, p. 22-29.

Foster, E. R., and Savage, R. J., 1989. Methods of historical shoreline analysis. *Coastal Zone '89*, New York: American Society of Civil Engineers, p. 4434-4448.

Kaye, C. A., 1959. Shoreline features and Quaternary shoreline changes, Puerto Rico: Washington, D.C., *U.S. Geological Survey Professional Paper 317-B*, p. 49-140.

Morelock, J., 1978. *Shoreline of Puerto Rico*: San Juan, Puerto Rico, Department of Natural Resources, 45 p.

Morelock, J., 1984. Coastal erosion in Puerto Rico: *Shore and Beach*, v. 52, no. 1, p. 18-27.

Morelock, J., 1987. Beach sand budget for western Puerto Rico: *Coastal Sediments '87*: New York, American Society of Civil Engineers, p. 1333-1345.

Pilkey, O. H., 1976. Surfing in Puerto Rico, *in* Pilkey, O. H., ed., *A Marine Atlas of Puerto Rico*: San German, Puerto Rico, M. J. Cerame-Vivas, Inc., p. 73-81.

The Surf Report, 1982. v. 3, no. 5, ISSN 0270-2630, 12 p.

Thieler, E. R., and Danforth, W. W., 1994a. Historical Shoreline Mapping (I): Improving Techniques and Reducing Positioning Errors: *Journal of Coastal Research*, v. 10, no. 3, p. 549-563.

Thieler, E. R., and Danforth, W. W., 1994b. Historical Shoreline Mapping (II): Application of the Digital Shoreline Mapping and Analysis Systems (DSMS/DSAS) to Shoreline Change Mapping in Puerto Rico: *Journal of Coastal Research*, v. 10, no. 3, p. 600-620.

Thieler, E. R., and Danforth, W. W., 1993. *Historical Shoreline Changes in Puerto Rico, 1901-1987*: U.S. Geological Survey Open-File Report No. 93-574, 267 p., 39 plates.

Turner, M. D., 1956. Some geologic aspects of the beaches and beach erosion in Puerto Rico: *Shore and Beach*, v. 24, no. 2, p. 4-8.

FIGURE CAPTIONS

Fig. 1) The island of Puerto Rico is the smallest and easternmost of the Greater Antilles. The study area, near the town of Rincón, is located on the northwestern coast.

Fig. 2) The study area described in this report extends from Punta Higüero to Punta Cadena. These rocky headlands form the boundaries of the Rincón-Córcega littoral cell defined by Morelock (1987). Roads are shown in black, creeks and canals in gray. The numbered points are the locations of GPS-surveyed ground control points used for aerotriangulation adjustments of the historical aerial photography.

Fig. 3) Much of the shoreline between Punta Higüero and Punta Cadena is part of a low-lying alluvial plain fronted by a sandy beach. The beach near Córcega, in the southern part of the study area, is shown here.

Fig. 4) From Punta Higüero to Punta Ensenada, the beach is underlain by beachrock, eolianite and metasedimentary rocks. Here, a beachrock deposit, characterized by low-angle, seaward-dipping planar bedding, forms the seaward end of a small tombolo. At different locations in this reach of shoreline, the beachrock sits unconformably on either eolianite or metasedimentary rocks. These three units comprise a low-relief terrace across which a relatively small prism of sand (the active beach) moves in response to seasonal changes in wave energy and long-term erosion.

Fig. 5) At Punta Ensenada, a small marina (top of photo) was constructed in 1983. The marina entrance includes a breakwater/jetty system. The breakwaters and periodic dredging activities at the marina are probably having a profound effect on recent shoreline erosion rates. (See text for discussion.)

Fig. 6) Shoreline erosion at Rincón has resulted in the construction of small seawalls and revetments in front of threatened buildings. The revetment shown here is partially covered by trucked-in sand and loose construction debris.

Fig. 7) Two field surveys of wet/dry shoreline position were conducted in February and August of 1994 using a backpack-mounted GPS receiver. The receiver logged positions at 5-second intervals as the backpacker walked along the wet/dry line. The GPS data were real-time and post-processed for differential correction, yielding a horizontal accuracy of about 2-3 meters. The rocky shoreline near Punta Cadena is shown here.

Fig. 8) The four methods used to calculate the shoreline rates-of-change for each transect in this study. The data points represent the distance from the baseline for each shoreline on a particular date. (From Dolan *et al.*, 1991)

Fig. 9) The shoreline in the study area can be divided into four distinct reaches based on the erosion rates in Table 1. The histograms show the long-term (44 years) rate-of-change for each reach, as expressed by the *aor* statistic. Negative values indicate erosion. The map shows the numbered transect locations along the shoreline. Measurement transects are indicated by the short, shore-perpendicular lines. The transect line-length gives and indication of the relative magnitude of shoreline movement between 1950-1994. (See text for discussion.)

Fig. 10) This histogram shows the difference in end-point erosion rates for Reach C. Numbered transect locations correspond to those shown in Figure 8. Over the past seven years, erosion rates in the northern portion of the reach have increased dramatically relative to the

rates recorded between 1950-1977. In the southern half of Reach C, the erosion rate has actually decreased over the period 1987-1994 (Table 3). (See text for discussion.)

Fig. 11) There is a well-developed scarp present along much of the southern portion of Reach C. This photo shows a two-meter high scarp cut into unconsolidated, sandy alluvial sediments. The fresh scarp face, hanging roots, and lack of talus at the scarp base indicate a very rapid rate of erosion. The data indicate that this area is experiencing about 4-6 m/yr of shoreline erosion. The cow, however, appears unconcerned.

Fig. 12) The beach in the southern part of Reach C is wide, and appears "healthy" (large sand volume, no large active scarps or exposed tree roots). This is in spite of an erosion rate of nearly 1.0 m/yr. This apparent health is probably due to an increased sediment supply coming from accelerated erosion in Reach B. Part is also surely due to the timing of the photograph itself (taken at the end of the fair-weather summer period).